

Assessing uncertainties in landslide susceptibility predictions in a changing environment (Styrian Basin, Austria)

Raphael Knevels¹, Helene Petschko¹, Herwig Proske², Philip Leopold³, Aditya N. Mishra⁴, Douglas Maraun⁴, and Alexander Brenning¹

¹Department of Geography, Friedrich Schiller University Jena, Jena, 07743, Germany

²Remote Sensing and Geoinformation Department, JOANNEUM RESEARCH Forschungsgesellschaft mbH, Graz, 8010, Austria

³Centre for Low-Emission Transport, AIT Austrian Institute of Technology GmbH, Vienna, 1210, Austria

⁴Wegener Centre for Climate and Global Change, Regional Climate Research Group, Karl-Franzens-University Graz, Graz, 8010, Austria

Correspondence: Raphael Knevels (raphael.knevels@uni-jena.de)

S1 Supplemental Figures

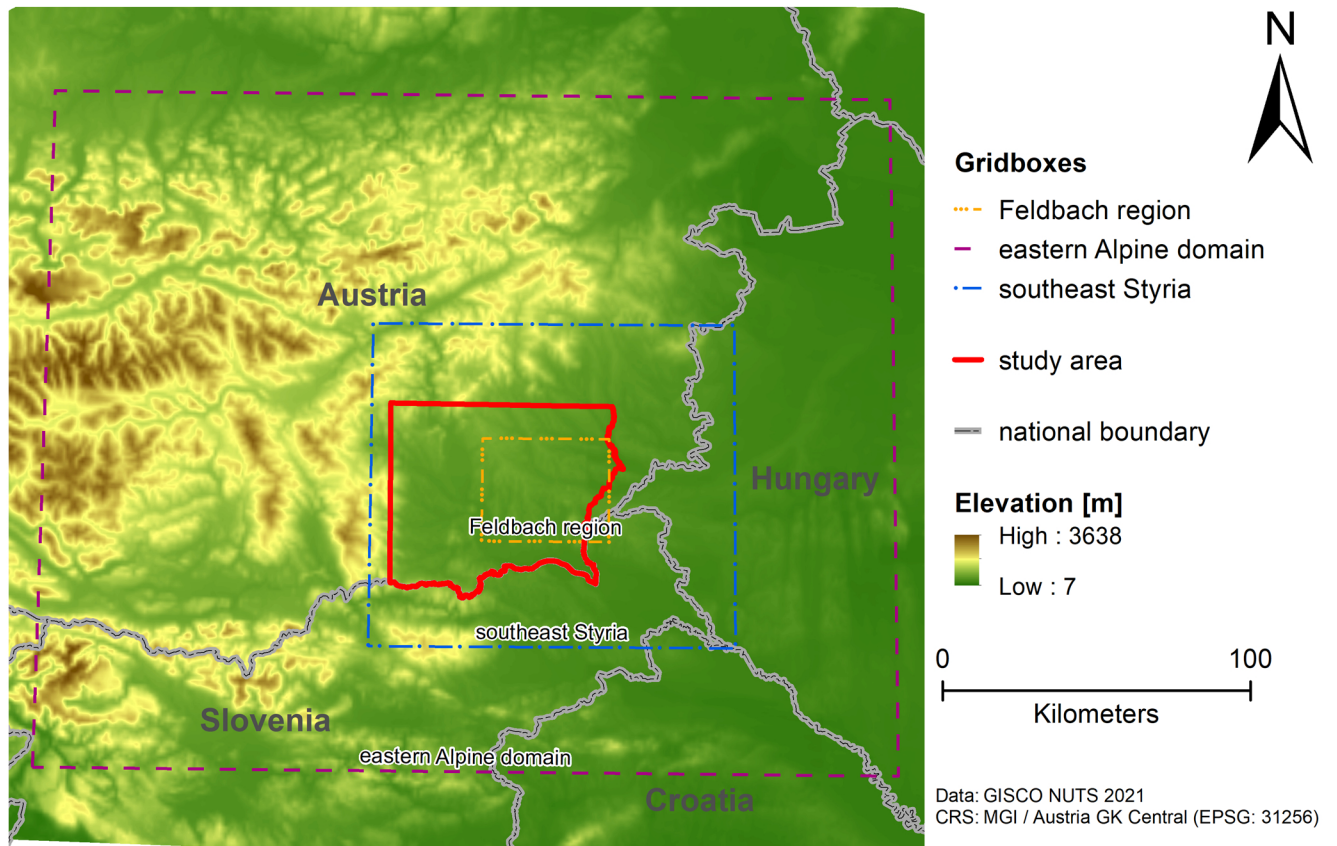


Figure S1. Delta change domains. Precipitation values were based on eastern Alpine domain (Maraun et al. (2022) and this study). Soil moisture values were based on the Feldbach region in Maraun et al. (2022) but on southeast Styria in this study.

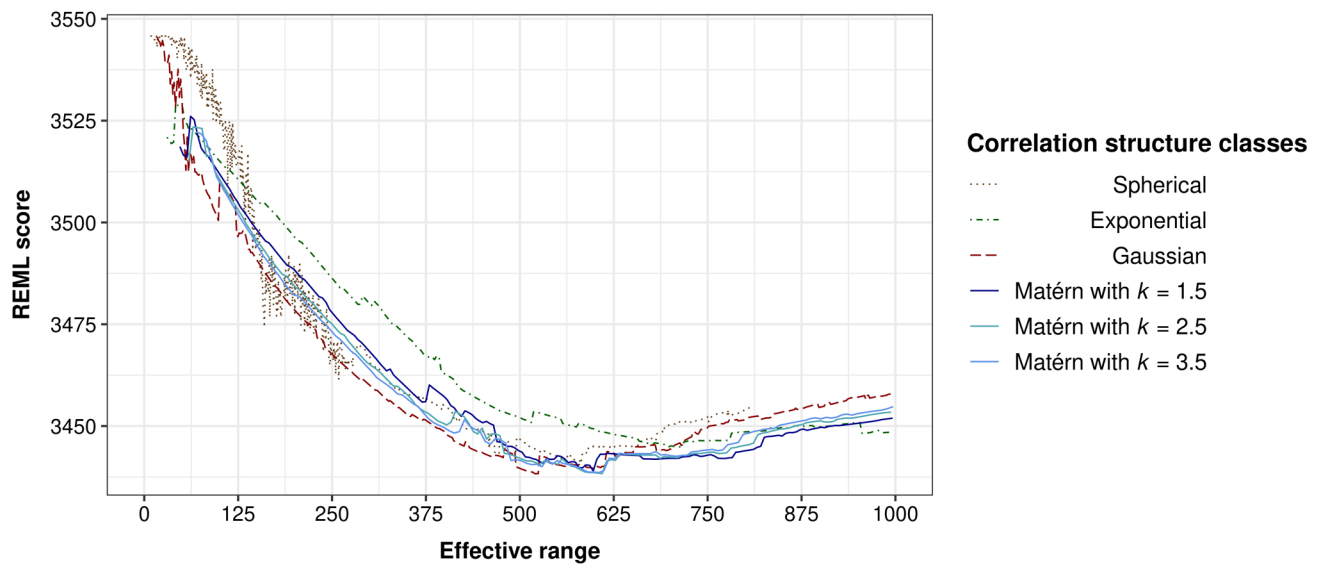


Figure S2. Optimization result for a Gaussian Process (GP) smoother with different correlation functions and effective ranges.

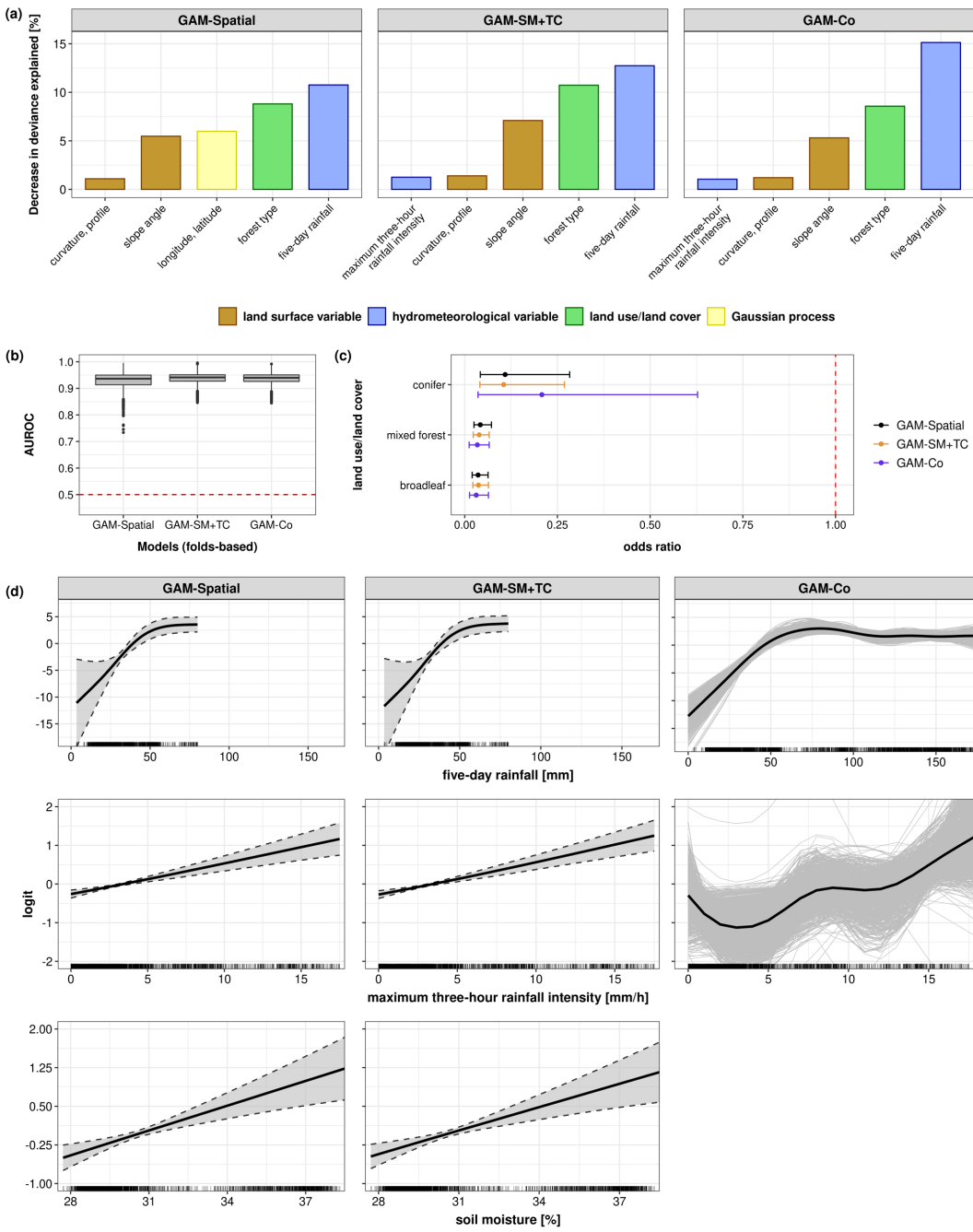


Figure S3. Model diagnostics. (a) Top five most important variables sorted by mean decrease in deviance explained [%]. For an overview of all input variables, refer to Table A6. (b) Comparison of model performances (folds-based). (c) Comparison of predictor-response relationships of land use/land cover (LULC) variables using odds ratios. (d) Comparison of predictor-response relationships of hydrometeorological variables. Note: The y axes in (d) are plot-dependent. Estimates and predictor-response relationships for GAM-Co are based on SpCV models in Knevels et al. (2020). In grey: 95 % pointwise Bayesian credible intervals.

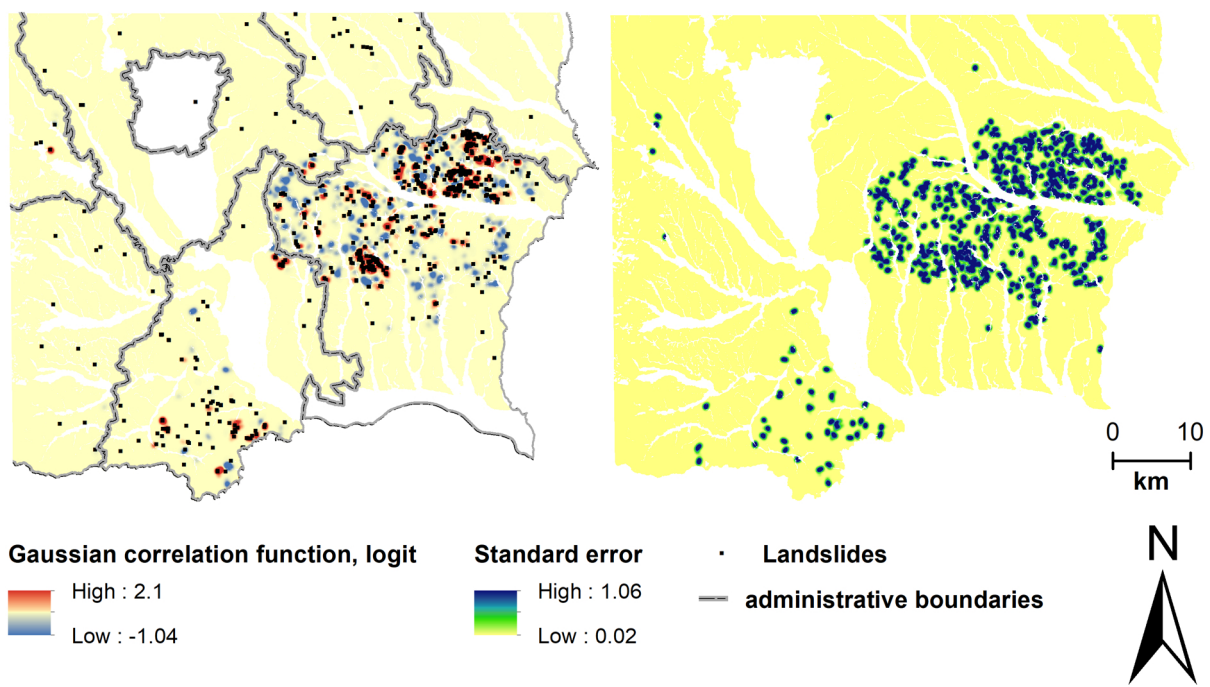


Figure S4. Relationship of GP smoother to landslide occurrences.

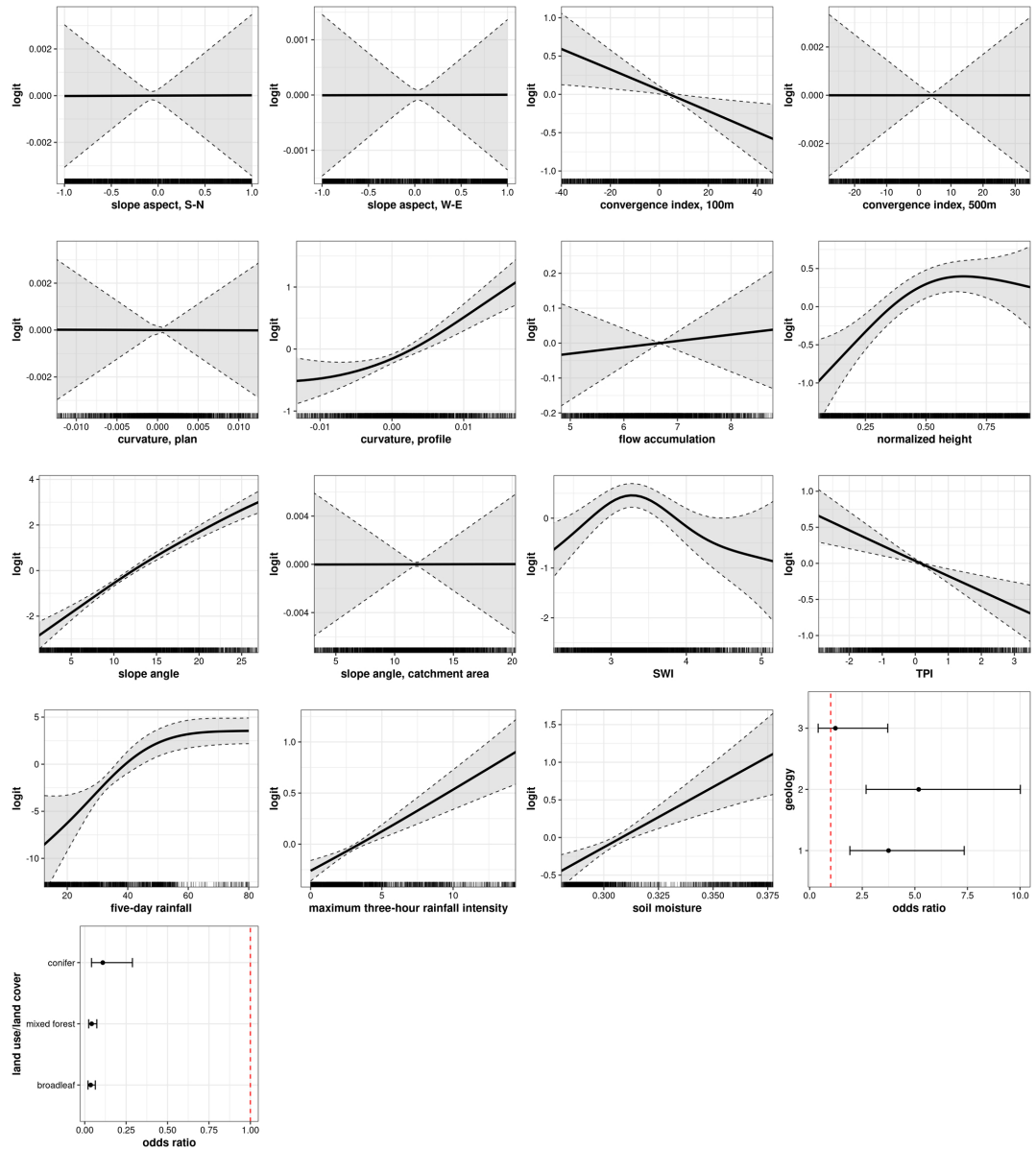


Figure S5. Predictor-response relationships of GAM-Spatial. Grey: 95% pointwise Bayesian credible interval. Reference level of LULC 2015: ‘Forest’; Lithological units: Reference: ‘Neogene formations with coarse-grained layers’, 0: ‘Neogene formations dominated by fine-grained sediments’, 1: ‘pre-Würmian Pleistocene formations’. Note: the y axes are plot-dependent, and the x axes of non-parametric transformation functions are limited to the 5th and 95th percentile. For the predictor-response relationship of the GP smoother, please refer to Fig. S3.

S2 Supplemental Tables

Table S1. Uncertainty of predicted landslide susceptible area

Scenario	GFDL	GFDL LULC	HadGem	HadGEM LULC	IPSL	IPSL LULC	MIROC	MIROC LULC
Low Susceptibility (present-day: 79.1 [75; 82.5])								
NO-CC	78.5 [73.9; 82.3]		80.1 [75.5; 84.0]		79.2 [74.8; 83.0]		79.4 [74.9; 83.3]	
PARIS	79.5 [74.8; 83.5]	80.4 [75.7; 84.3]	78.7 [73.8; 82.8]	79.6 [74.7; 83.6]	79.5 [74.6; 83.6]	80.4 [75.6; 84.3]	79.0 [74.2; 83.0]	79.9 [75.1; 83.8]
3 K	82.6 [77.2; 87.3]	83.4 [78.2; 88.0]	77.0 [71.6; 81.7]	78.0 [72.6; 82.4]	85.6 [78.1; 91.4]	86.4 [79.1; 91.8]	78.4 [72.3; 83.2]	79.3 [73.2; 83.9]
4 K	82.3 [77.1; 86.5]	83.2 [78.1; 87.2]	75.7 [69.8; 80.6]	76.6 [70.7; 81.3]	82.0 [74.9; 87.5]	82.8 [75.8; 88.2]	77.8 [70.8; 83.3]	78.7 [71.8; 84.1]
Medium Susceptibility (present-day: 16.0 [13.3; 19.0])								
NO-CC	16.4 [13.4; 19.6]		15.4 [12.5; 18.7]		16.0 [13.0; 19.2]		15.9 [12.9; 19.1]	
PARIS	15.7 [12.7; 19.1]	15.3 [12.3; 18.6]	16.3 [13.1; 19.7]	15.8 [12.7; 19.2]	15.7 [12.7; 19.1]	15.2 [12.3; 18.7]	16.1 [13.0; 19.4]	15.6 [12.6; 18.9]
3 K	13.9 [10.4; 17.6]	13.3 [9.9; 17.1]	17.1 [13.7; 20.6]	16.6 [13.3; 20.3]	11.6 [7.4; 16.8]	11.1 [7.0; 16.2]	16.3 [12.9; 20.1]	15.8 [12.5; 19.7]
4 K	14.0 [10.9; 17.6]	13.5 [10.4; 17.1]	17.7 [14.3; 21.4]	17.3 [13.9 ;21.0]	14.0 [10.3; 18.6]	13.5 [9.7; 18.1]	16.5 [12.9; 20.6]	16.0 [12.4 ;20.2]
High Susceptibility (present-day: 4.9 [3.8; 6.3])								
NO-CC	5.1 [3.8; 6.8]		4.4 [3.2; 6.1]		4.8 [3.6; 6.4]		4.7 [3.5; 6.3]	
PARIS	4.7 [3.4; 6.5]	4.3 [3.1; 5.9]	5.1 [3.7; 6.9]	4.6 [3.4; 6.3]	4.7 [3.4; 6.6]	4.3 [3.1; 6.0]	5.0 [3.6; 6.8]	4.5 [3.3; 6.2]
3 K	3.6 [2.1; 5.4]	3.3 [1.9; 4.9]	5.9 [4.1; 8.2]	5.4 [3.8; 7.6]	2.7 [1.3; 5.0]	2.5 [1.1; 4.6]	5.4 [3.5; 8.0]	4.9 [3.2; 7.4]
4 K	3.7 [2.4; 5.4]	3.3 [2.2; 4.9]	6.6 [4.6; 9.3]	6.1 [4.2; 8.7]	4.0 [2.2; 6.7]	3.7 [2.0; 6.2]	5.7 [3.5; 8.9]	5.3 [3.2; 8.4]

Note: Area relative to total study area. 95 % CI are based on within-event internal climate model variability and parametric landslide model uncertainty. Susceptibility classes are based on observed landslide occurrences: low 5 %, medium 25 % high 30 %.

Table S2. Odds ratios of landslide occurrences of comparable susceptibility classes relative to present-day landslide susceptibility

Scenario	GFDL	GFDL LULC	HadGem	HadGEM LULC	IPSL	IPSL LULC	MIROC	MIROC LULC
Low Susceptibility								
NO-CC	1.05		0.93		1.00		0.99	
	[1.01; 1.09]		[0.89; 0.96]		[0.96; 1.04]		[0.94; 1.03]	
PARIS	0.96	0.92	1.03	0.99	0.96	0.92	1.00	0.96
	[0.93; 1.01]	[0.89; 0.96]	[0.98; 1.08]	[0.94; 1.04]	[0.92; 1.00]	[0.89; 0.96]	[0.97; 1.04]	[0.93; 1.00]
3 K	0.75	0.72	1.15	1.10	0.55	0.53	1.03	0.99
	[0.69; 0.79]	[0.66 ;0.76]	[1.08; 1.22]	[1.03; 1.17]	[0.52; 0.58]	[0.50; 0.55]	[0.97; 1.10]	[0.93; 1.05]
4 K	0.77	0.74	1.27	1.21	0.76	0.73	1.06	1.02
	[0.73; 0.80]	[0.70; 0.76]	[1.18; 1.37]	[1.13; 1.31]	[0.72; 0.82]	[0.69; 0.78]	[0.98; 1.15]	[0.94; 1.10]
Medium Susceptibility								
NO-CC	1.05		0.92		0.99		0.98	
	[1.00; 1.09]		[0.88; 0.96]		[0.95; 1.04]		[0.93; 1.02]	
PARIS	0.96	0.95	1.04	1.02	0.97	0.95	1.01	1.00
	[0.92; 1.01]	[0.91; 1.00]	[0.98; 1.09]	[0.96; 1.08]	[0.92; 1.01]	[0.91; 1.00]	[0.97; 1.06]	[0.96; 1.04]
3 K	0.75	0.75	1.18	1.16	0.57	0.57	1.06	1.05
	[0.68; 0.79]	[0.67; 0.79]	[1.09; 1.26]	[1.08; 1.23]	[0.54; 0.61]	[0.54; 0.61]	[0.99; 1.14]	[0.98; 1.13]
4 K	0.77	0.76	1.31	1.28	0.80	0.80	1.11	1.10
	[0.73; 0.8]	[0.73; 0.79]	[1.20; 1.42]	[1.18; 1.39]	[0.75; 0.86]	[0.74; 0.86]	[1.02; 1.21]	[1.01; 1.19]
High Susceptibility								
NO-CC	1.05		0.91		0.98		0.96	
	[1.00; 1.10]		[0.87; 0.96]		[0.93; 1.03]		[0.92; 1.01]	
PARIS	0.97	0.95	1.04	1.03	0.97	0.96	1.02	1.01
	[0.92; 1.02]	[0.91; 1.01]	[0.98; 1.11]	[0.96; 1.09]	[0.92; 1.03]	[0.91; 1.02]	[0.97; 1.07]	[0.96; 1.06]
3 K	0.75	0.74	1.22	1.20	0.60	0.60	1.11	1.10
	[0.67; 0.8]	[0.66; 0.79]	[1.12; 1.32]	[1.1; 1.3]	[0.55; 0.65]	[0.55; 0.65]	[1.02; 1.22]	[1.01; 1.21]
4 K	0.77	0.76	1.37	1.35	0.85	0.85	1.20	1.19
	[0.73; 0.81]	[0.72; 0.8]	[1.24; 1.52]	[1.23; 1.5]	[0.78; 0.93]	[0.78; 0.93]	[1.08; 1.33]	[1.08; 1.32]

Note: 95 % CI are based on within-event internal climate model variability. Susceptibility classes are based on observed landslide occurrences: low 5 %, medium 25 % and high 70 %.

Table S3. Ratio of uncertainty sources in predicted landslide susceptibility

Scenario	GFDL	GFDL LULC	HadGem	HadGEM LULC	IPSL	IPSL LULC	MIROC	MIROC LULC
Low Susceptibility <i>Within-event intern climate variability to landslide model uncertainty Climate scenario to landslide model uncertainty</i>								
NO-CC	0.15 ± 0.23		0.15 ± 0.23		0.17 ± 0.23		0.18 ± 0.23	
PARIS	0.15 ± 0.23	0.16 ± 0.24	0.19 ± 0.23	0.19 ± 0.24	0.15 ± 0.23	0.15 ± 0.23	0.14 ± 0.23	0.14 ± 0.23
3 K	0.22 ± 1.12	0.22 ± 1.14	0.22 ± 1.13	0.22 ± 1.16	0.10 ± 0.78	0.10 ± 0.81	0.20 ± 1.03	0.20 ± 1.04
4 K	0.14 ± 0.91	0.14 ± 0.93	0.26 ± 0.89	0.27 ± 0.91	0.15 ± 0.68	0.15 ± 0.7	0.22 ± 0.73	0.22 ± 0.74
Medium Susceptibility								
NO-CC	0.11 ± 0.17		0.12 ± 0.17		0.13 ± 0.18		0.14 ± 0.18	
PARIS	0.12 ± 0.18	0.12 ± 0.18	0.14 ± 0.18	0.14 ± 0.18	0.11 ± 0.18	0.12 ± 0.17	0.10 ± 0.18	0.11 ± 0.17
3 K	0.19 ± 0.97	0.19 ± 0.97	0.15 ± 1.00	0.15 ± 0.99	0.09 ± 0.70	0.09 ± 0.71	0.15 ± 0.96	0.15 ± 0.95
4 K	0.12 ± 0.70	0.12 ± 0.70	0.17 ± 0.7	0.18 ± 0.70	0.13 ± 0.58	0.13 ± 0.57	0.16 ± 0.64	0.16 ± 0.63
High Susceptibility								
NO-CC	0.20 ± 0.28		0.18 ± 0.28		0.20 ± 0.29		0.22 ± 0.29	
PARIS	0.19 ± 0.30	0.20 ± 0.34	0.24 ± 0.30	0.25 ± 0.33	0.19 ± 0.29	0.20 ± 0.32	0.18 ± 0.29	0.18 ± 0.31
3 K	0.25 ± 1.28	0.27 ± 1.46	0.29 ± 1.07	0.29 ± 1.15	0.13 ± 1.02	0.13 ± 1.11	0.26 ± 0.97	0.27 ± 1.05
4 K	0.15 ± 1.23	0.16 ± 1.38	0.34 ± 0.92	0.35 ± 1.00	0.19 ± 0.86	0.20 ± 0.95	0.27 ± 0.77	0.28 ± 0.82

Susceptibility classes are based on observed landslide occurrences: low 5%, medium 25% and high 70%.

References

- Knevels, R., Petschko, H., Proske, H., Leopold, P., Maraun, D., and Brenning, A.: Event-Based Landslide Modeling in the Styrian Basin, Austria: Accounting for Time-Varying Rainfall and Land Cover, *Geosciences*, 10, 217, <https://doi.org/10.3390/geosciences10060217>, number: 6 Publisher: Multidisciplinary Digital Publishing Institute, 2020.
- Maraun, D., Knevels, R., Mishra, A. N., Truhetz, H., Bevacqua, E., Proske, H., Zappa, G., Brenning, A., Petschko, H., Schaffer, A., Leopold, P., and Puxley, B. L.: A severe landslide event in the Alpine foreland under possible future climate and land-use changes, *Communications Earth & Environment*, 3, 1–11, <https://doi.org/10.1038/s43247-022-00408-7>, number: 1 Publisher: Nature Publishing Group, 2022.